Raman and FTIR studies of the structural aspects of Nasicon-type crystals; $AFeTi(PO_4)_3$ [A = Ca, Cd]

M. Junaid Bushiri[a],*, C.J. Antony[a], Abderrahim Aatiq[b]

[a]Department of Physics, University of Kerala, Kariavattom, Trivandrum, Kerala-695 581, India
[b]Faculté des Sciences Ben M'Sik, Département de Chimie, LCMS, Av. Idriss El harti, B.P. 7955, Casablanca, Morocco

Abstract

Raman and FTIR spectra of $CaFeTi(PO_4)_3$ and $CdFeTi(PO_4)_3$ are recorded and analyzed. The observed bands are assigned in terms of vibrations of TiO_6 octahedra and PO_4 tetrahedra. The symmetry of TiO_6 octahedra and PO_4 tetrahedra is lowered from their free ion symmetry. The presence of Fe^{3+} ion disrupts the Ti–O–P–O–Ti chain and leads to the distortion of TiO_6 octahedra and PO_4 tetrahedra. The PO_4^{3-} tetrahedra in both crystals are linearly distorted. The covalency bonding factor of PO_4^{3-} polyanion of both the crystals are calculated from the Raman spectra and compared to that of other Nasicon-type systems. The numerical values of covalency bonding factor indicates that there is a reduction in redox energy and cell voltage and is attributed to strong covalency of PO_4^{3-} polyanionin.
© 2008 Elsevier Ltd. All rights reserved.

Keywords: C. Infrared spectroscopy; C. Raman spectroscopy

1. Introduction

Phosphates with general formula $ABB'(PO_4)_3$ crystallize mainly in the Nasicon $NaZr_2(PO_4)_3$-type structure. Materials with this family possess a rhombohedral $R\bar{3}c$ structure and have many technological applications due to its superionic conductivity, chemical stability and high catalytic activity. The $ABB'(PO_4)_3$ Nasicon-type phase consists of a $BB'(PO_4)_3$ framework built up by a corner-sharing $B(B')O_6$ octahedra and PO_4 tetrahedra. In this structure each octahedron is surrounded by six tertrahedra and each tetrahedron is connected to four octahedra. This family of compounds possess 'open' structures in which alkali ions can move with significantly reduced activation barriers and hence potential for applications as fast ion conductors [1–8]. B sites can be accommodated with large number of transition as well as non-transition metals. The tetravalent and trivalent redox couples in B site can give technically

attractive battery voltage [5]. The phosphate polyanions can lowers the open circuit voltage of isostructural compounds [5]. Recently, considerable importance has attained for phosphate with Nasicon-type framework with elements like Ti, Fe, Nb, Sn, etc. which can have more than one oxidation state [6]. The partial substitution of tetravalent element like Ti with trivalent element like Al was very effective for enhancement of ionic conductivity of these materials [7]. Several works have been reported to study the relationship between the structural and electrochemical properties of potential materials for battery applications [5,7,9]. Aatiq et al. studied the structure of $AFeTi(PO_4)_3$ [A = Ca, Cd] with aid of powder X-ray diffraction data using the Rietveld method [6]. Since Ca^{2+} and Ti^{4+} ions are isoelectronic, these cannot be distinguished without ambiguity by XRD. But the analysis of Ca–O and Fe(Ti)–O distances permits to conclude about cationic distribution of $CaFeTi(PO_4)_3$. Apart from this, the solid electrolytic properties of materials are usually caused by features of their atomic structure. The vibrational spectra of these materials will provide additional information on the nature of fast ion transport in solids [10]. In the present study the internal structure of the title compounds

*Corresponding author. Present address: Department of Physics, Cochin University of Science and Technology, Kochi, Kerala 682022, India. Tel.: +91 0484 2577404.

E-mail address: junaidbushiri@gmail.com (M. Junaid Bushiri).

are investigated by using Raman and FITR spectra. Further an attempt is made to determine the redox energy and cell voltage of title compounds from the Raman spectral data.

2. Experimental

Powder crystalline samples of $CaFeTi(PO_4)_3$ and $CdFe-Ti(PO_4)_3$ abbreviated as CaFT and CdFT, respectively were prepared by solid state reaction technique from the mixtures of TiO_2, Fe_2O_3, carbonates $CaCO_3$ or $CdCO_3$ and $NH_4H_2PO_4$ [6]. Bruker RFS 100/S spectrometer was used to record the Raman spectra in the stokes region. The FTIR spectra of the compounds were recorded using a Bruker IFS-66v-FTIR spectrometer in the region $400–4000 \, cm^{-1}$ by KBr Pellet method.

3. Factor group analysis

The structure of both CaFT and CdFT crystals are having Nasicon-type framework structure and crystallizes in hexagonal system with space group $R\bar{3}c$ (D_{3d}^6). Its unit cell parameters are: $a = 8.518(1) \, Å$, $c = 21.797(2) \, Å$ and $a = 8.534(1) \, Å$, $c = 21.416(2) \, Å$, for CaFT and CdFT, respectively [6]. In the crystal structure, two Ca(Cd) atoms are in the D_3 site, the Fe and Ti atoms each two in number are, respectively, occupying C_{3i} and C_i sites. Six P atoms are located at C_2 site and all the 24 oxygen atoms are found to occupy the C_1 site. The vibrational modes of these compounds are obtained by the group theoretical method [11]. The total irreducible representation excluding acoustic modes are distributed as

$$\Gamma_{105} = 10A_{1g} + 12A_{2g} + 13E_g + 12A_{1u} + 13A_{2u} + 16E_u.$$

4. Results and discussion

4.1. Vibrational analysis

The crystal structure of CaFT is built up by corner sharing of $Ti(Fe)O_6$ octahedra and PO_4 tetrahedra in such a way that each octahedra is surrounded by six tetrahedra (Fig. 1). Within Nasicon framework, there are interconnected interstitial sites, usually labeled as M1 and M2, through which a cation can diffuse. Ca^{2+} ions in CaFT are considered to be distributed within the M1 sites whereas the M2 site is empty (Fig. 1). The structure of CdFT is similar to the previous one, in which the M1 sites are filled with Cd ions. The crystal structure refinement suggests that, Fe^{3+} ions are occupying the Ti sites [6]. Considering chemical nature of both Fe^{3+} and Ti^{4+} ions there is a probability of different types of Fe/Ti–O bonds. Hence the TiO_6 octrahedra are disturbed by the presence of Fe^{3+} ions in the site. Moreover the ionic radii of these ions are almost identical ($r_{Fe} = 0.6454 \, Å$; $r_{Ti} = 0.605 \, Å$) [6]. The Ti–O bond length is weak and varies from 1.902 to 2.041 Å in CaFT and from 1.897 to 2.044 Å in CdFT. There will be
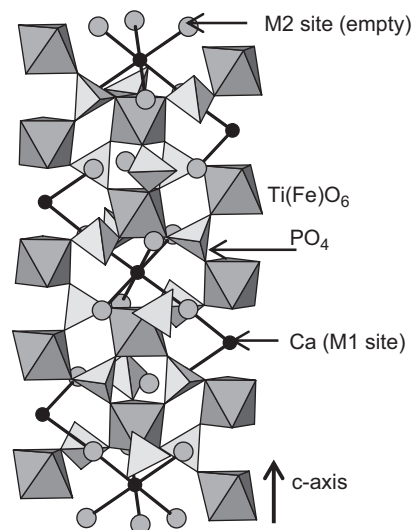

Fig. 1. Perspective view of the $CaFeTi(PO_4)_3$ Nasicon phase [6].

higher possibility of Fe ions disturbing Ti–O–P as well as Ti–O–Ti chain. This is due to the equivalence of Fe^{3+} and Ti^{4+} ions which occupy equivalent sites in the structure as reported in similar type compounds [12,13].

4.2. Vibrations of TiO_6 octahedra

In metal–oxide systems containing titanium, the binding forces within the metal–oxygen octahedra are higher than the crystal binding forces. External modes usually appear at lower frequencies than internal modes [14]. The free ion TiO_6 octahedra with O_h symmetry has six fundamental modes of vibration, viz, symmetric stretching mode v_1 (A_{1g}), asymmetric stretching modes v_2 (E_g) and v_3 (F_{1u}), asymmetric bending mode v_4 (F_{1u}), symmetric bending mode v_5 (F_{2g}) and the Raman and IR inactive mode v_6 (F_{2u}). The v_1, v_2, and v_5 modes are Raman active, whereas the v_3 and v_4 modes are IR active [15–17]. The TiO_6 octahedral modes were reported to be at $v_1 = 639$, $v_2 = 519$, $v_3 = 513$, $v_4 = 399$, $v_5 = 197$, and $v_6 = 144 \, cm^{-1}$ in TiO_2 crystals [18]. In compounds having Ti–O–Ti chain v_1 mode of TiO_6 octahedra are observed around $700 \, cm^{-1}$ as in $KTiOPO_4$, $Na(TiO)PO_4$ and $(TiO)_2P_2O_7$ [16,17,19]. But the symmetric stretching mode of TiO_6 octahedron is reported around $900 \, cm^{-1}$ in $NaLnTiO_4$ and at $891 \, cm^{-1}$ in $Na_5Ti(PO_4)_3$. This is interpreted due to the strong nature of Ti–O bonds [1,20]. The PO_4 stretching modes are reported above $950 \, cm^{-1}$ in Nasicon-type compounds like $NaZr_2(PO_4)_3$, $Na_3NiZr(PO_4)_3$, and $Na_3MgZr(PO_4)_3$ [21]. It is interesting to note in the present study, the v_3 PO_4 modes of CaFT and CdFT are observed at higher frequency than that of titanyl and niobyl phosphates [12,16,17,19]. This observation suggests an increasing covalent character in Ti–O bond of CaFT and CdFT in comparison to that of titanyl phosphate [22]. Further, Ti–O symmetric stretching (v_1) vibration is expected to have the strongest intensity in the Raman spectra. This spectral behavior is reported in

many perovskite-like crystals or substances containing MO, groups such as $SnNbO$, $BiNbO_4$, and $LaCuO$ [14,23–25]. According to the previously mentioned reports, the relatively strong band observed in the Raman spectra at 928 (CaFT) and at 926 (CdFT) cm^{-1} are assigned to v_1 mode of TiO_6 octahedra. Apart from these intense Raman bands, strong IR bands are also observed at 932 (CaFT) and at 915 (CdFT) cm^{-1} in the v_1 mode region. The relatively weak bands in the Raman spectra at 670 in CaFT and at 672 cm^{-1} in CdFT are attributed to v_2 mode of TiO_6 octahedra. Very strong Raman bands observed at 310 and 309 cm^{-1} in both the compounds are due to v_5 modes of TiO_6 octahedra. The remaining bands are assigned in Table 1. The moderately strong Raman bands at 220 (CaFT) and 224 cm^{-1} (CdFT) are contributed to the Raman and IR inactive v_6 mode. The charge redistribution, or Ti-shift within the TiO_6 octahedra should strongly affect the frequency of modes involving Ti–O stretching [26]. The octahedral substitutution of Fe^{3+} has led to a distortion of the structure, which is in agreement with similar compounds having Nasicon structure [7]. If the stretching frequency of the shortest metal–oxygen bond is observed in the lower wavenumber side, the MO_6 octahedral structure is more regular especially in metal–oxide systems [27]. In the present study TiO_6 stretching frequencies (i.e., v_1, v_2, and v_3 modes) are shifted considerably to higher wavenumber side as compared to that of TiO_2 crystal. Further, the activation of v_1 mode in the IR spectra, v_2 and v_6 modes

in the Raman spectra, suggests that TiO_6 octahedral symmetry is lowered and distorted in both compounds. The observed distortion of TiO_6 octahedra may be related to the incorporation of Fe^{3+} ions in the Ti site [6].

4.3. Vibrations of PO_4 tetrahedra

The vibrations of free PO_4 tetrahedra with T_d symmetry have four fundamental modes. These frequency modes fall at v_1 (A_1) 938, v_2 (E) 420, v_3 (F_2) 1017, and v_4 (F_2) 567 cm^{-1}. All the modes are Raman active whereas v_3 and v_4 ones are IR active only [9,15,16,28]. The v_1 mode region of PO_4 tetrahedra in CaFT shows a strong and broad band extending from 965 to 1014 with peak at 984 cm^{-1} (Fig. 2 and Table 1). Similarly, in CdFT a strong and broad band extending from 956 to 1005 with a peak at 974 cm^{-1} is observed (Fig. 2). The corresponding region in the IR spectra also has bands (Fig. 3). The IR spectrum in the triply degenerate asymmetric stretching v_3 mode region of CaFT has four bands at 1049, 1068, 1117, and 1227 cm^{-1} where as CdFT shows bands at 1047, 1076, 1118, and 1226 cm^{-1}. The Raman spectra of both the samples show

Table 1

Raman and FTIR spectral data and band assignments of CaFeTi(PO₄)₃ and CdFeTi(PO₄)₃

CaFeTi(PO_4)$_3$		CdFeTi(PO_4)$_3$		Assignments
Raman	IR	Raman	IR	
82 w		84 w		
169 ms		175 ms		Ti translational
201 ms		204 ms		
220 ms		224 ms		v_6 TiO_6
249 sh				
310 vs		309 vs		v_5 TiO_6 and FeO_6
436 vs		437 vs	418 w	v_2 PO_4 and v_4 TiO_6
457 vs	447 ms	455 ms	455 m	
			473 sh	
534 vw	547 w	532 vw	539 vw	v_3 TiO_6
566 vw	562 w	563 vw		
583 vw		581 vw	580 vw	v_4 PO_4
	646 ms		642 ms	v_2 TiO_6
670 vw		672 vw		v_2 TiO_6
928 vvs	932 vs	926 vvs	915 vs	v_1 TiO_6
984 vs	1002 vs	974 vs	989 vs	v_1 PO_4
1056 sh	1049 sh	1040 sh	1047 vs	
	1068 s		1076 vs	
1089 ms				v_3 PO_4
	1117 vs	1101 ms	1118 vs	
1194 vw			1196 vw	
	1227 ms		1226 ms	

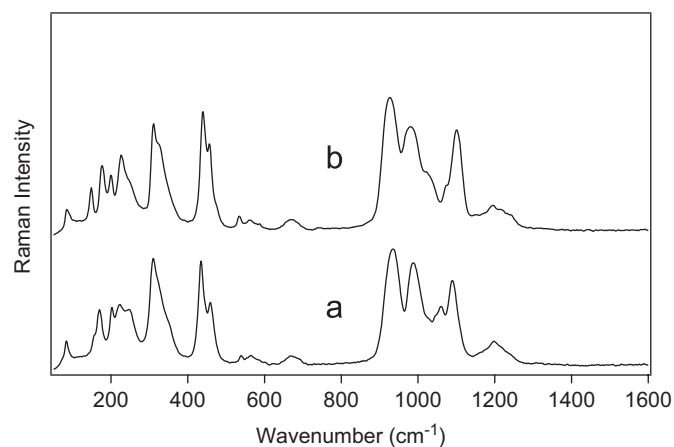vw—very weak; w—weak; sh—shoulder; ms—moderately strong; vvs—very very strong, s—strong.

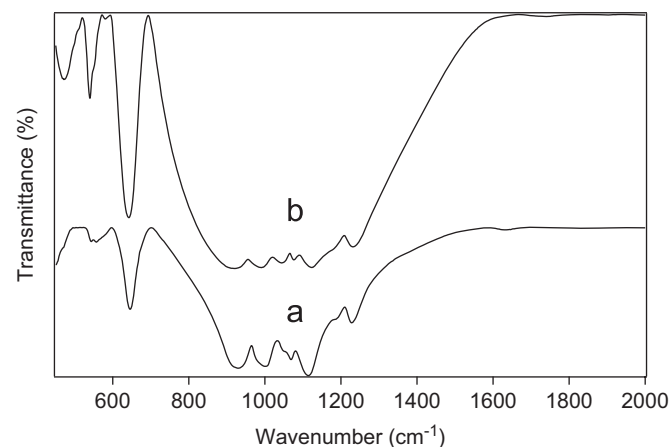Fig. 2. Raman spectra of (a) CaFeTi(PO_4)$_3$ and (b) CdFeTi(PO_4)$_3$.

Fig. 3. FTIR spectra of (a) CaFeTi(PO_4)$_3$ and (b) CdFeTi(PO_4)$_3$.

bands in the above region (Fig. 2, Table 1). These values are close to those already reported in the literature for Nasicon-like phosphates [1,3,9,10,22,29]. In CaFT, P–O distances are 1.520 and 1.527 Å with a mean P–O distance of 1.523 Å. But in CdFT, P–O distances are 1.501 and 1.547 with a mean P–O distance of 1.523 Å [6]. Popovic et al. have formulated the following empirical relation connecting P–O bond lengths and stretching frequencies [30]:

$$v = 224,500\exp(-R/28.35), \tag{1}$$

where R is the P–O bond lengths in pm. By replacing P–O distance values in the above expression, the obtained values are given in Table 2. These values are relatively comparable with that of the experimentally obtained one and this further confirm that the bands observed in the Raman Spectra at 928 (CaFT) and at 926 (CdFT) cm^{-1} are due to v_1 mode of TiO$_6$ octahedra.

The relatively strong bands observed in the Raman spectrum of CaFT correspond to doubly degenerate v_2 mode vibration of PO$_4$ tetrahedra and appears at 436 and 457 cm^{-1}. Similarly the Raman spectrum of CdFT also shows bands at 437 and 455 cm^{-1}. The degeneracy of this mode is found to be lifted in both the compounds. IR spectra of these samples also have bands in the aforesaid region (Fig. 3 and Table 1). Note that the above-described spectral patterns are almost similar to that of Nasicon structures reported in literature. Assignments of v_4 mode of PO$_4$ tetrahedra are not obvious, since it overlaps with the v_3 modes of TiO$_6$ octahedra [16,17]. The observed lifting of degeneracies of v_2 and v_3 modes in the IR spectra implies that the symmetry of PO$_4$ tetrahedra is lowered from its free ion T_d symmetry. Further, the presence of symmetric stretching and bending modes in the IR spectra also confirms the above result.

The P–O bond lengths vary considerably between the two compounds even though the mean bond lengths are the same (Table 2). The stretching frequency of CdFT is shifted towards the low wavenumber side of the order of 10 cm^{-1}

as compared to that of CaFT. This is probably due to comparatively longer P–O distance (1.547 Å) in CdFT as reported [6]. The splitting of v_3 mode of PO$_4$ tetrahedra is of the order of 159 cm^{-1} in CaFT and 180 cm^{-1} in CdFT. This observation suggests that distortion of PO$_4$ tetrahedra is more in CdFT than in CaFT. The appearance of the symmetric stretching mode at a higher frequency than that of the regular tetrahedra indicates linear distortion of the PO$_4$ tetrahedra in both the compounds. Generally, Raman bands originated from the vibrations of PO$_4$ stretching modes are relatively weak in most of the crystals like KTiOPO$_4$, SbOPO$_4$, MoPO$_5$, NbOPO$_4$, etc. due to the presence of Met–O–Met–O chain. Strong bands may also occur in the Raman spectra depending on Ti atoms environment [24,25,32]. But in the present study, the appearance of intense bands corresponds to PO$_4$ stretching modes which rules out the possibility of the Met–O–Met–O chain [19]. A broader Raman band profile is observed for both compounds in the symmetric stretching region of PO$_4$ tetrahedra and is about 49 cm^{-1}. This broad band profiles suggest that there is a disorder in structure of samples under investigation [12,14,21,31]. The presence of Fe^{3+} ions in Ti site induces a disorder around the PO$_4$ tetrahedra because the PO$_4$ tetrahedra are linked by corners to Fe/TiO$_6$ octahedra [6].

Materials with these framework are useful for battery applications and hence it is worthwhile to determine covalency strength of PO$_4$ tetrahedra. It is of interest to note that the cell voltage depends on the redox couple of the transition metal atoms and it related to redox energy and covalency strength. The covalency strength of PO$_4$ tetrahedra is directly linked to the material structure. The vibrational spectra are sensitive to the covalency of the phosphate group, the covalency strength can be estimated by the following expression [9]:

$$\Delta = (v_1 - v_2)/(v_1 + v_2). \tag{2}$$

The covalency strength parameter of PO$_4^{3-}$ polyanion is found to be 0.38 in CaFT and 0.37 in CdFT. This covalency bonding factor is comparable to that of orthophosphate group of compounds. The higher covalency bonding factor of PO$_4$ polyanion in CaFT and CdFT indicates that a reduction in redox energy and cell voltage as compared to that of diphosphates and Nasicon-type systems reported in the literature [9]. The decrease in redox energy is attributed to the presence of PO$_4^{3-}$ polyanion with strong covalency bonding factor which reduces the strength of Met–O covalency in the structure [9].

4.4. Other bands

Bands observed below 200 cm^{-1} are mostly due to rotational and translational modes. These bands are influenced by the replacement of the Ca by Cd. This can be attributed to external lattice modes in which the Ca^{2+} (or Cd^2) ions move with respect to the PO$_4$ and TiO$_6$, groups. Further vibrations contributed by FeO$_6$ octahedra

Table 2
Bond lengths and stretching wavenumbers calculated (*$v = 224,500\exp(-R/28.35)$) with experimental values of CaFT and CdFT

Name of compoud	P–O bond length (pm)	Stretching wavenumbers (exp.) Raman (cm^{-1})	Stretching wavenumbers (cal.)*(cm^{-1})
CaFT	152	1056	1054
	152.7	984	1028
	152.3 (Mean P–O)	1056	1043
CdFT	150.1	1101	1127
	154.7	974	958
	152.4 (Mean P–O)	1040	1039

are expected in the 300–400 cm^{-1} region [1,3]. Unambiguous assignments of these bands are limited. The band observed at 175 cm^{-1} in the Raman spectrum of CdFT and at 169 cm^{-1} in CaFT may be due to Ti translational mode as reported by Barj et al. [33].

5. Conclusions

The symmetry of both TiO_6 octrahedra and PO_4 tetrahedra is lowered from its free ion symmetry and are corner-shared in CaFT and CdFT crystals. The presence of Fe^{3+} ion disrupts the Ti–O–P–O–Ti chain within the Nasicon structure. The PO_4 tetrahedra is linearly distorted in $CaFeTi(PO_4)_3$ and $CdFeTi(PO_4)_3$. The broader band profiles of PO_4 tetrahedra suggest that there is a disordered structure in the samples under investigation. The calculated higher covalency bonding factor of PO_4 polyanion in CaFT and CdFT indicates that a reduction in redox energy as well as cell voltage as compared to that of diphosphates and certain Nasicon-type systems. The decrease in redox energy is attributed to the presence of PO_4^{3-} polyanionin with strong covalency.

References

[1] K.J. Rao, K.C. Sobha, A. Sundeepkumar, Infrared and raman spectroscopic studies of glasses with NASICON-type chemistry, Proc. Indian Acad. Sci. 113 (2001) 497–514.

[2] Iara F. Gimenez, Oswaldo L. Alves, Formation of a novel polypyrrole/porous phosphate glass ceramic nanocomposite, J. Braz. Chem. Soc. 10 (1999) 167–168.

[3] G. Butt N. Sammes, G. Tompsett, A. Smirnova, O. Yamamoto, Raman spectroscopy of superionic Ti-doped $Li_3Fe_2(PO_4)_3$, and $LiNiPO_4$ structures, J. Power Sources 134 (2004) 72–79.

[4] S. Zhang, B. Quan, Z. Zhao, B. Zhao, Y. He, W. Chen, Preparation and characterization of NASICON with a new sol–gel process, Mater. Lett. 58 (2003) 226–229.

[5] K.S. Nanjundaswamy, A.K. Padhi, J.B. Goodenough, S. Okada, H. Ohtsuka, H. Arai, J. Yamaki, Synthesis, redox potential evaluation and electrochemical characteristics of NASICON-related-3D framework compounds, Solid State Ion. 92 (1996) 1–10.

[6] A. Aatiq., H. Dhoum, Structure of $AFeTi(PO_4)_3$(Ä = Ca, Cd) Nasicon phases from powder X-ray data, Powder Diffr. 19 (2004) 157–161.

[7] M. Cretin, P. Fabry, L. Abello, Study of $Li_{1+x}Al_xTi_{2-x}(PO_4)_3$ for Li^+ potentiometric sensors, J. Eur. Ceram. Soc. 15 (1995) 1149–1156.

[8] G.Le. Polles, J-J. Videau, R. Olazcuaga, Analyse structurale par spectroscopie Raman et Infrarouge de quelques phosphates de cuivre detype Nasicon, J. Solid State Chem. 127 (1996) 341–349.

[9] C.M. Julien, P. Jozwiak, J. Garbarczyk, Vibrational spectroscopy of electrode materials for rechargeable lithium batteries—IV. Lithium metal phosphates, in: Proceedings of the International Workshop "Advanced Techniques for Energy Sources Investigation and Testing, Sofia, Bulgaria, September 2004.

[10] V.V. Kravchenko, V.I. Michailov, S.E. Sigaryov, Some features of vibrational spectra of $Li_3M_2(PO_4)_3$(M = Sc, Fe) compounds near a superionic phase transition, Solid State Ion. 50 (1992) 19–30.

[11] W.G. Fateley, F.R. Dollish, N.T. Mc Devitt, F.F. Bentley, Infrared and Raman Selection Rules for Molecular and Lattice Vibrations—The Correlation Method, Wiley, New York, 1972.

[12] M.J. Bushiri, V.U. Nayar, Structural aspects of $KMg_{1/3}Nb_{2/3}PO_5$ a KTP analogue—Raman and FTIR spectroscopic study, J. Nonlinear Opt. Phys. Mater. 10 (2001) 343–345.

[13] E.M.Mc. Carron III, J.C. Calabrese, J.E. Gier, L.K. Cheng, C.M. Foris, J. D . Bierlein, A structural comparison of aliovalent analogues: $K(Mg_{1/3}Nb_{2/3})PO_5$ and $KTiOPO_4$, J. Solid State Chem. 102 (1993) 354–361.

[14] A. Hushur, J.-H. Ko, S. Kojima, Raman scattering study of A- and B-site substitutions in ferroelectric $Bi_4Ti_3O_{12}$, J. Korean Phys. Soc. 41 (2002) 763–768.

[15] K. Nakamoto, Infrared and Raman Spectra of Inorganic and Coordination Compounds—Part A, fifth ed., Wiley-Interscience, New York, 1997.

[16] G.E. Kugel, F. Brehat, B. Wyncke, M.D. Fontana, G. Marnier, C. Carabatos-Nedelec, J. Mangin, The vibrational spectrum of a $KTiOPO_4$, single crystal studied by Raman and infrared reflectivity spectroscopy, J. Phys. C: Solid State Phys. 21 (1988) 5565–5583.

[17] M.J. Bushiri, V.U. Nayar, Raman and FTIR spectroscopic studies of potassium titanylphosphate ($KTiOPO_4$) doped with lanthanum and praseodymium, Ind. J. Phys. 75B (2) (2001) 109–116.

[18] K. Vivekanandan, S. Selvasekarapandian, P. Kolandaivel, M.T. Sebastian, S. Suma, Raman and FT-IR spectroscopic characterisation of flux grown $KTiOPO_4$ and $KRbTiOPO_4$ non-linear optical crystals, Mater. Chem. Phys. 49 (1997) 204–210.

[19] G.E. Bamberger, G.M. Begun, O.B. Cavin, Synthesis and characterization of sodium–titanium phosphates, $Na_4(TiO)(PO_4)_2$, $Na(TiO)PO_4$, and $NaTi_2(PO_4)_3$, J. Solid State Chem. 73 (1988) 317–324.

[20] G. Blasse, G.P.M. Van Den Heuvel, Vibrational spectra and structural considerations of compounds $NaLnTiO_4$, J. Solid State Chem. 10 (1974) 206–210.

[21] M. Chakir, A.EI. Jazouli, D.de. Waal, Synthesis crystal structure and spectroscopy properties of $Na_3AZr(PO_4)_3$(A = Mg, Ni) and $Li_{2.6}Na_{0.4}NiZr(PO_4)_3$ phosphates, J. Solid State Chem. 179 (2006) 1883–1891.

[22] M. Ma, A.W. Kowska, J. Hanuza, Crystal structure and vibrational properies of $Rb_2MgWO_2(PO_4)_2$—a new framework phosphate, J. Solid State Chem. 179 (2006) 103–110.

[23] N. Wakiya, J. Shiihara, K. Shinozaki, N. Mizutani, Raman spectroscopic determination of pyrochlore-type compound on the synthesis and decomposition of sol–gel-derived $Pb(Mg_{1/3}Nb_{2/3})O_3(PMN)$, J. Solid State Chem. 142 (1999) 344–348.

[24] E. Husson, F. Genet, A. Lachgar, Y. Piffard, The vibrational spectra of some antimony phosphates, J. Solid State Chem. 75 (1988) 305–312.

[25] M. Issac, Investigations on the Raman and infrared spectra of certain molybdates, Ph. D. Thesis, University of Kerala, 1992.

[26] N. Kolev, R.P. Bontchev, A.J. Jacobson, V.N. Popov, V.G. Hadjiev, A.P. Litvinchuk, M.N. Iliev, Raman spectroscopy of $CaCu_3Ti_4O_{12}$, Phys. Rev. B 66 (2002) 132102–132104.

[27] F.D. Hardcastle, I.E. Wachs, Determination of molybdenum–oxygen bond distances and bond orders by Raman spectroscopy, J. Raman Spectrosc. 21 (1990) 683–691.

[28] M.J. Bushiri, M. Fakhfakh, R.S. Jayasree, V.U. Nayar, Raman and infrared spectral analysis of thallium niobyl phosphates $Tl_2NbO_2PO_4$, $Tl_3NaNb_4O_9(PO_4)_2$ and $TlNbOP_2O_7$, J. Mater. Chem. Phys. 73 (2002) 179–185.

[29] R. Pikl, D. de Waal, A. Aatiq, A. El Jazouli, Vibrational spectra and factor group analysis of $Mn_{(0.5+x)}Ti_{(2-2x)}Cr_{2x}(PO_4)_3$ $\{0 \leqslant x \leqslant 0.50\}$, Vibr. Spectrosc. 16 (1998) 137–143.

[30] L. Popovic, D. de Waal, J.C.A. Boeyens, Correlation between Raman wavenumbers and P–O bond lengths in crystalline inorganic phosphates, J. Raman Spectrosc. 36 (2005) 2–11.

[31] A.A. Belik, A.P. Malakho, P.S. Salamakha, B.I. Lazoryak, Magnetic and vibrational properties and crystal structure of $Sr_{9.2}Co_{1.3}(PO_4)_7$ with disordered arrangements of some strontium, cobalt, and phosphate ions, J. Solid State Chem. 179 (2006) 161–168.

[32] G.T. Stranford, R.A. Condrate Sr., The vibrational spectra of α-$MoPO_5$ and α-$NbPO_5$, J. Solid State Chem. 52 (1984) 248–253.

[33] M. Barj, H. Perthuis, P. Colomban, Relations between sublattice disorder, phase transitions and conductivity in NASICON, Solid State Ion. 9–10 (1983) 845–850.